

Molecular Logic Gates and Switches Based on 1,3,4-Oxadiazoles Triggered by Metal Ions

Ai-Fang Li, Yi-Bin Ruan, Qian-Qian Jiang, Wen-Bin He, and Yun-Bao Jiang*^[a]

Abstract: Organic molecular devices for information processing applications are highly useful building blocks for constructing molecular-level machines. The development of “intelligent” molecules capable of performing logic operations would enable molecular-level devices and machines to be created. We designed a series of 2,5-diaryl-1,3,4-oxadiazoles bearing a 2-(*para*-substituted)phenyl and a 5-(*o*-pyridyl) group (substituent X = NMe₂, OEt, Me, H,

and Cl; **1a–e**) that form a bidentate chelating environment for metal ions. These compounds showed fluorescence response profiles varying in both emission intensity and wavelength toward the tested metal ions Ni²⁺, Cu²⁺, Zn²⁺, Cd²⁺, Hg²⁺, and Pb²⁺ and the respons-

Keywords: bidentate ligands • chelates • fluorescence • metal ions • molecular devices

es were dependent on the substituent X, with those of **1d** being the most substantial. The 1,3,4-oxadiazole O or N atom and pyridine N atom were identified as metal-chelating sites. The fluorescence responses of **1d** upon metal chelation were employed for developing truth tables for OR, NOR, INHIBIT, and EnNOR logic gates as well as “ON-OFF-ON” and “OFF-ON-OFF” fluorescent switches in a single 1,3,4-oxadiazole molecular system.

Introduction

Molecular systems capable of performing logic operations are attractive for the construction of molecular-level devices and machines that are in high demand in information technology.^[1,2] Since the first report of photonic molecular AND logic gates,^[3] logic systems consisting of chemically encoded information as input and a fluorescence signal as output have received considerable attention and molecular systems showing functions such as AND, NAND, OR, NOR, XOR, XNOR, and INHIBIT have been widely explored.^[4,5] However, relatively few molecular systems capable of performing multiple logic functions of superior information processing capability have been reported.^[6] In general, the reported systems were based on the modulation of the emission properties of the designed molecules by different combinations of external inputs, such as metal ions, solution pH, and sol-

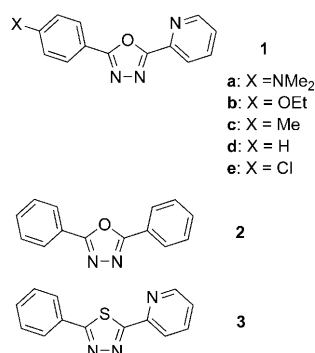
vent polarity.^[6] The tailored design of molecules exhibiting multiple logic functions therefore remains to be explored. It appears that “intelligent” molecules with distinct coordination behavior could be potential candidates for the construction of novel logic operations,^[7] which would allow the functions to be activated by the same kinds of metal-ion inputs. We envisaged that a fluorescent ligand with varying metal-chelating ability and chelating mode, with its emissive state capable of modulation as well, would allow multiple logic gates to be created from a single fluorescent ligand by using individual metal ions or a combination of them as the input, with fluorescence output in terms of both intensity and wavelength.

1,3,4-Oxadiazoles are organic molecules known for their excellent optical properties, and are thus extensively exploited as signaling components in molecular sensory systems.^[8] We proposed to employ 1,3,4-oxadiazole as the molecular framework for constructing multiple fluorescent logic gates and switches. This was based on the conjugated structure of 2,5-diaryl-1,3,4-oxadiazole, such that its electronic distribution and emissive state can be modulated by varying the substituent at the 2-phenyl ring. Meanwhile, this structural framework allows a bidentate metal-chelating environment to be established when a metal binding site is incorporated into the 5-aryl ring. As the O and N atoms in the 1,3,4-oxadiazole moiety can be respectively combined with this additional binding site, two options of the bidentate chelation

[a] Dr. A.-F. Li, Y.-B. Ruan, Q.-Q. Jiang, W.-B. He, Prof. Y.-B. Jiang
Department of Chemistry, College of Chemistry
and Chemical Engineering
and the MOE Key Laboratory of Analytical Sciences
Xiamen University, Xiamen 361005 (China)
Fax: (+86) 592-2185662
E-mail: ybjiang@xmu.edu.cn

Supporting information for this article is available on the WWW under <http://dx.doi.org/10.1002/chem.200903265>.

may be created. We therefore designed a series of 2,5-diaryl-1,3,4-oxadiazoles bearing a 2-(*para*-substituted)phenyl and a 5-(*o*-pyridyl) group (substituent X = NMe₂, OEt, Me, H, and Cl; **1a–e**, respectively; Scheme 1). The *o*-pyridyl



Scheme 1. Molecular structure of 2,5-diaryl-1,3,4-oxa(thio)diazoles **1–3**.

group at the C5 position of the oxadiazole ring was expected to couple with the 1,3,4-oxadiazole ring to form an (O, N) or (N, N) bidentate chelation environment for metal ions, whereas the 2-phenyl group was introduced to test if the electronic distribution and the emissive state could be tuned by way of substitution. We found that the emission of **1a–e** was indeed highly sensitive to the substitution, and the response profiles in terms of emission intensity and wavelength toward the tested metal ions Ni²⁺, Cu²⁺, Zn²⁺, Cd²⁺, Hg²⁺, and Pb²⁺ varied quite a lot, depending on the substituent X. On the basis of these observations, we developed a unique molecular system capable of performing multiple logic functions (OR, NOR, INHIBIT, and EnNOR) as well as “ON-OFF-ON” and “OFF-ON-OFF” fluorescent switches by simply varying the combination and level of metal-ion inputs in a single fluorescent ligand **1d**. To the best of our knowledge, this is the first molecular system capable of performing multiple logic functions based on the 1,3,4-oxadiazole fluorophore.

Results and Discussion

Crystal structure of 1b: Figure 1 shows the crystal structure of **1b**, which confirms the planar structure of the 2,5-diaryl-

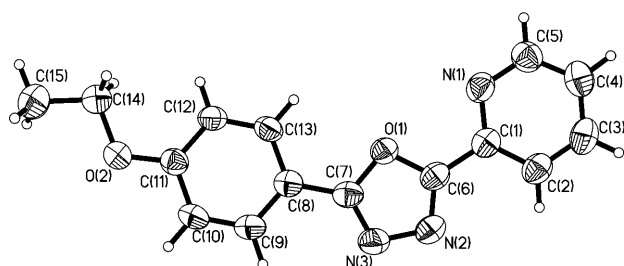


Figure 1. Crystal structure of **1b**.

1,3,4-oxadiazole fluorophore. This provides support to the molecular design strategy that the electronic distribution may be tuned by substitution at the 2-phenyl ring and by metal chelation to the rest of the molecule as well.

Absorption and fluorescence spectra of 1: The absorption spectra of **1a–e** were recorded in solvents of increasing polarity, namely, cyclohexane (CHX), diethyl ether (DEE), ethyl acetate (EtOAc), dichloromethane (CH₂Cl₂), and acetonitrile (CH₃CN). Some of the spectral parameters are summarized in Table S1 in the Supporting Information. In general, the absorption of **1a** and **1b–e** exhibits a major band at 340 and 287–309 nm, respectively (Figure 2; Fig-

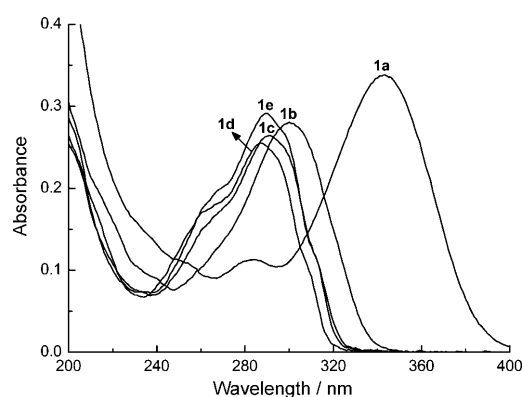


Figure 2. Absorption spectra of **1a–e** (10 μM) in CH₃CN.

ures S1–S4 and Table S1 in the Supporting Information). The significantly redshifted absorption of **1a** compared to that of **1b–e** (Figure 2) is presumably due to the strong electron-donating ability of the NMe₂ substituent. Molar absorption coefficients at the 10⁴ M⁻¹ cm⁻¹ order of magnitude are indicative of the π→π* transition character. It was found, from the data compiled in Table S1 (Supporting Information), that the absorption of **1** underwent a redshift with increasing electron-donating ability of the substituent X in the same solvent, whereas the absorption of **1** was insensitive to the solvent polarity.

The fluorescence of **1a–e** experiences a similar redshift with increasing electron-donating ability of X in the same solvent (Table S1 in the Supporting Information). However, the emission of **1a–e** was found to be influenced by the solvent polarity to an extent depending on X (Figure 3). The emission of **1a** shows a significant redshift with increasing solvent polarity from 388 nm in CHX to 525 nm in CH₃CN, which is in contrast to the solvent-polarity-insensitive nature of the absorption spectrum. This observation reveals that the emissive state of **1a** is of a charge-transfer (CT) type. Upon the same variation of solvent, the emission of **1b** and **1c** shifts to the red by 39 and 13 nm, respectively, whereas that of **1d** and **1e** hardly changes its position (Figure 3). The observation that the solvatochromic effect becomes less and less with decreasing electron-donating ability of X in **1** indicates that the CT in **1**, if any, occurs from the X-substituted

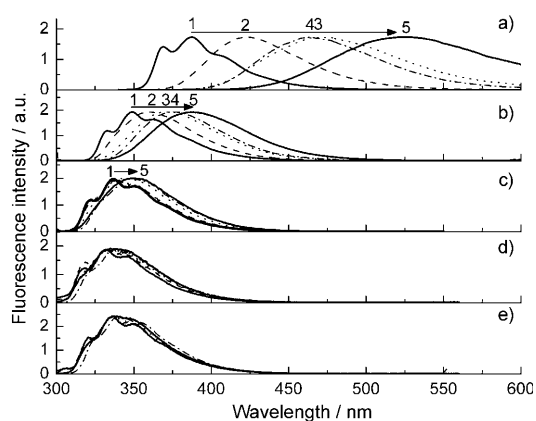


Figure 3. Normalized fluorescence spectra of **1a–e** (spectra a–e, respectively) in CHX (1), DEE (2), EtOAc (3), CH₂Cl₂ (4), and CH₃CN (5).

2-phenyl group to the electron-deficient oxadiazole moiety. Fluorescence quantum yields of **1** (Table S1 in the Supporting Information) were sensitive to the electronic character of X, too. For example, quantum yields in CHX decreased dramatically from 0.71 (X=OEt) to 0.11 (Me), 0.015 (H), and 0.047 (Cl).

All these spectral properties confirm that the fluorescence of **1** is highly sensitive to the substituent X or the electronic distribution in the whole molecule, and the emissive state of **1** also undergoes variation with X. It was therefore expected that metal chelation to the bidentate structure formed by 1,3,4-oxadiazole and the 5-(*o*-pyridyl) moiety would act as an alternative way of tuning the electronic distribution and emission of the fluorescent ligands. In accordance with this assumption, we observed that the fluorescence quantum yield of **1d** in CH₃CN (0.015) was much lower than that (0.83) of its model compound **2**, in which the 5-(*o*-pyridyl) moiety in **1d** was replaced by a 5-phenyl group (Scheme 1). This suggests that when a metal ion binds to the pyridine N atom in **1d**, for example, chelation-induced fluorescence enhancement would be observed. It was hence made clear that the emission of a sophisticatedly chosen member of **1** could be employed to construct metal-ion-triggered molecular logic gates or fluorescent switches.

Absorption and fluorescence spectra of **1** in the presence of metal ions:

Interaction of **1** with metal ions was probed by the absorption and fluorescence responses of **1** in CH₃CN toward the tested metal ions Ni²⁺, Cu²⁺, Zn²⁺, Cd²⁺, Hg²⁺, and Pb²⁺ (Table 1). It was found that **1a–e** responded similarly in their absorption spectra toward these metal ions (Figures S5–S9 in the Supporting Information). The appearance of isosbestic points in the titration traces suggested the formation of well-defined binding complexes between **1a–e** and the tested metal ions, which thereby allows their binding constants (K_s) to be fitted by a nonlinear fitting procedure for a 1:1 binding complex^[9] (Table 1). In general, the K_s values of **1a–e** in CH₃CN became lower when substituent X was more electron-withdrawing. The fluorescence response profiles of **1a–e** toward these metal ions, however, were

Table 1. Absorption and fluorescence spectral parameters of **1** and **3** in the presence of 25 equivalents of metal ions in CH₃CN.

	Absorption			Fluorescence		
	λ_{abs} [nm]	ϵ [$10^4 \text{ M}^{-1} \text{ cm}^{-1}$]	K_s [10^5 M^{-1}] ^[a]	λ_{fla} [nm]	I/I_0 ^[b]	Φ ^[c]
1a	235/284/ 343	1.27/1.11/3.35	–	525	–	0.477
1a +Ni ²⁺	293/320/ 382	1.52/1.74/2.35	> 10 ¹	528	0.01	0.005
1a +Cu ²⁺	321/376/ 630	1.95/1.34/0.22	> 10 ¹	526	0.002	0.024
1a +Zn ²⁺	292/320/ 378	1.50/1.79/2.22	1.27 ± 0.043	529	0.08	0.022
1a +Cd ²⁺	292/325/ 366	1.40/1.88/1.99	0.21 ± 0.005	526	0.21	0.074
1a +Hg ²⁺	296/325/ 392	1.62/2.11/1.85	> 10 ¹	517	0.002	0.002
1a +Pb ²⁺	292/325/ 371	1.53/2.13/2.01	0.66 ± 0.012	526	0.21	0.059
1b	300	2.81	–	388	–	0.781
1b +Ni ²⁺	322	2.23	4.33 ± 0.70	390	0.02	0.041
1b +Cu ²⁺	332	1.91	> 10 ¹	390	0.005	0.007
1b +Zn ²⁺	315	2.18	0.38 ± 0.007	508	0.65	0.511
1b +Cd ²⁺	309	2.19	0.06 ± 0.004	491	0.94	0.721
1b +Hg ²⁺	329	1.85	> 10 ¹	557	0.02	0.022
1b +Pb ²⁺	314	2.01	0.28 ± 0.006	389	0.19	0.385
1c	290	2.62	–	350	–	0.255
1c +Ni ²⁺	308	2.27	3.42 ± 0.41	352	0.03	0.006
1c +Cu ²⁺	314	2.02	> 10 ¹	350	0.01	0.004
1c +Zn ²⁺	301	2.27	0.28 ± 0.005	414	2.8	0.721
1c +Cd ²⁺	298	2.25	0.08 ± 0.008	403	1.6	0.386
1c +Hg ²⁺	312	1.90	> 10 ¹	452	0.30	0.031
1c +Pb ²⁺	301	2.05	0.22 ± 0.006	350	0.26	0.094
1d	287	2.57	–	334	–	0.015
1d +Ni ²⁺	301	2.30	1.42 ± 0.049	338	0.08	0.002
1d +Cu ²⁺	307	2.08	13.93 ± 3.12	334	0.05	0.002
1d +Zn ²⁺	296	2.33	0.22 ± 0.006	380	32.5	0.624
1d +Cd ²⁺	293	2.34	0.08 ± 0.007	377	11.5	0.239
1d +Hg ²⁺	306	2.02	> 10 ¹	416	0.42	0.009
1d +Pb ²⁺	296	2.07	0.18 ± 0.004	334	0.56	0.009
1e	289	2.94	–	337	–	0.044
1e +Ni ²⁺	303	2.60	1.24 ± 0.055	341	0.09	0.002
1e +Cu ²⁺	310	2.33	11.66 ± 2.75	344	0.04	0.002
1e +Zn ²⁺	299	2.63	0.17 ± 0.004	390	10.3	0.537
1e +Cd ²⁺	293	2.64	0.03 ± 0.003	387	4.0	0.194
1e +Hg ²⁺	308	2.27	> 10 ¹	429	0.15	0.011
1e +Pb ²⁺	298	2.46	0.13 ± 0.005	350	0.39	0.023
3	308	2.51	–	375	–	0.029
3 +Ni ²⁺	321	2.25	4.92 ± 0.74	375	0.04	0.003
3 +Cu ²⁺	329	2.02	> 10 ¹	375	0.01	0.003
3 +Zn ²⁺	319	2.26	0.32 ± 0.008	403	4.4	0.121
3 +Cd ²⁺	311	2.33	0.035 ± 0.003	395	2.3	0.059
3 +Hg ²⁺	325	2.02	> 10 ¹	424	0.41	0.013
3 +Pb ²⁺	311	2.23	0.064 ± 0.005	375	0.77	0.026

[a] Binding constant of metal ion. [b] Fluorescence enhancement factor, the ratio of fluorescence intensity in the presence of 25 equivalents of metal ion (I) to that in the absence of the metal ion (I_0). [c] Fluorescence quantum yields of **1a–e** and **3** in the presence of 25 equivalents of metal ion, measured by referring to quinine sulfate standard.^[10]

found to differ very markedly. The CT fluorescence of **1a** in CH₃CN was quenched by all the tested metal ions (Figure S10 in the Supporting Information). In contrast, the fluorescence of **1c–e** was quenched by Ni²⁺, Cu²⁺, Hg²⁺, and Pb²⁺, whereas it was enhanced by Zn²⁺ and Cd²⁺ (Figure 4 and Figures S11–S13 in the Supporting Information). With the latter two metal ions a redshifted new emis-

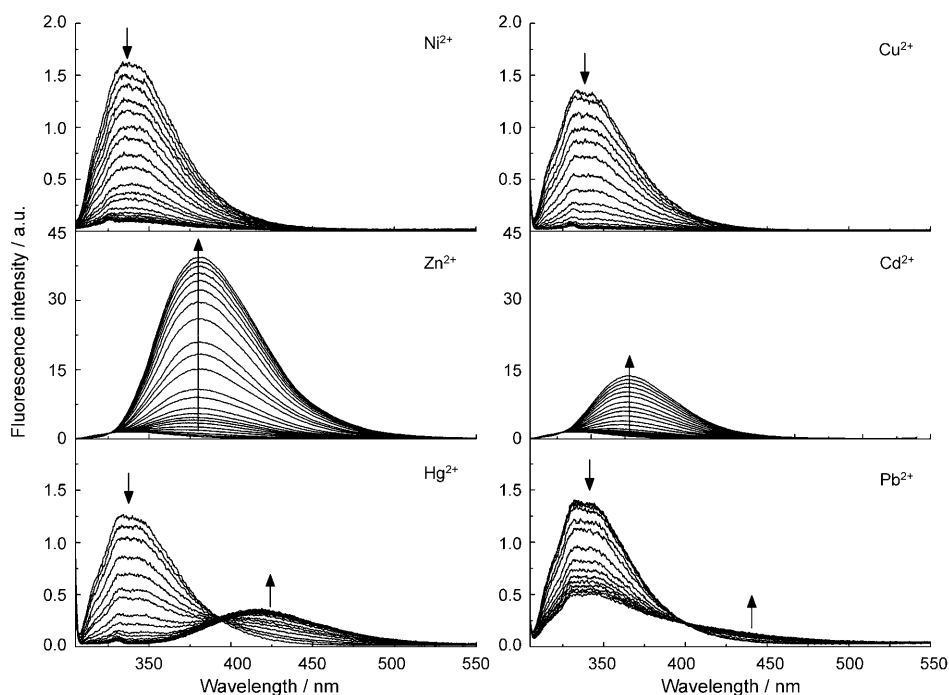


Figure 4. Fluorescence spectra of **1d** (10 μM) in CH_3CN in the presence of metal ions of increasing concentration. The concentration of metal ion increased as indicated by the arrows in the same manner from 0 to 250 μM . The excitation wavelengths for acquiring the fluorescence spectra of the tested metal ions Ni^{2+} , Cu^{2+} , Zn^{2+} , Cd^{2+} , Hg^{2+} , and Pb^{2+} were the isosbestic wavelengths of 296, 300, 296, 297, 300, and 299 nm, respectively.

sion band appeared together with an isoemissive point. It was also found that the redshifted band of **1b–e** in the presence of Zn^{2+} also depended on the substituent X (Figure S14 in the Supporting Information). The fluorescence response factors $(I-I_0)/I_0$ of **1a–e** in the presence of 25 equivalents of a given metal ion are plotted in Figure 5.

The results presented in Figures 4 and 5 reveal rich profiles of fluorescence response of **1** toward metal ions, in both intensity and wavelength. This again supports our molecular design of **1** and builds up the basis for constructing metal-ion-triggered logic gates and molecular switches using **1**. Our systematic investigation thus leads to the observation

that **1d** among **1a–e** shows the most pronounced fluorescence responses toward metal ions (Figure 5). This fact indicates that a subtle balance of the electronic characters of the 2- and 5-aryl groups is critical. Compound **1d** was therefore chosen for examining the logic functions. It should be emphasized that other metal ions, such as Na^+ , Mg^{2+} , and Ag^+ , were also tested and were found to exert practically no influence on the absorption and fluorescence of **1d** in CH_3CN (Figures S15–S17 in the Supporting Information). Related experiments were thereafter not continued on these three metal ions.

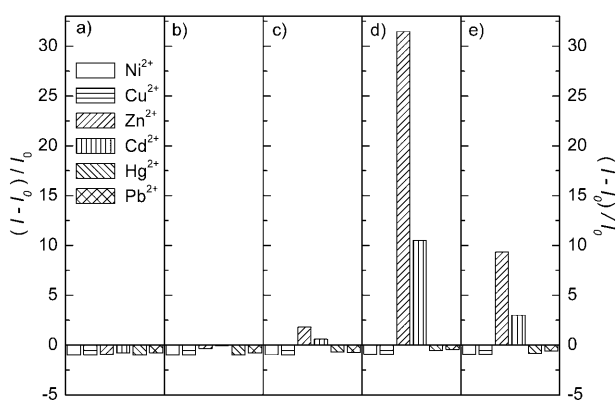


Figure 5. a–e) $(I-I_0)/I_0$ of **1a–e**, respectively, in CH_3CN in the presence of 25 equivalents of a given metal ion (250 μM). [**1a–e**] = 10 μM .

Coordination modes of 1 with metal ions: To probe the coordination modes of **1** toward metal ions, the absorption and fluorescence spectra of the tested molecule **1d** and control molecules **2** and **3** (Scheme 1) in CH_3CN in the presence of the tested metal ions were examined. The absorption and fluorescence spectra of **2**, which bears a 5-phenyl group rather than the 5-(*o*-pyridyl) group in **1d**, hardly showed any response toward the metal ions (Figures S18 and S19 in the Supporting Information), which indicates that the pyridine N atom in **1d** coordinates to the metal ions. With the control compound **3** that bears a 1,3,4-thiadiazole instead of the 1,3,4-oxadiazole in **1d**, the fluorescence response to Zn^{2+} in CH_3CN was much weaker than that of **1d**, whereas its responses to Cu^{2+} and Hg^{2+} were similar to those of **1d** (Figure 6 and Figure S20 in the Supporting Information). This finding suggests that the 1,3,4-oxadiazole O atom in **1d** dictates the fluorescence enhancement response of **1d**

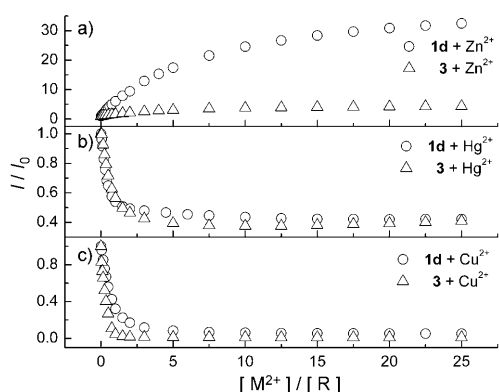


Figure 6. Plots of fluorescence enhancement factor (I/I_0) in CH_3CN versus concentration ratio of Zn^{2+} (a), Hg^{2+} (b), and Cu^{2+} (c) to **1d** and **3**. $[\mathbf{1d}] = [\mathbf{3}] = 10 \mu\text{M}$.

toward Zn^{2+} but not Cu^{2+} and Hg^{2+} . The slight difference in molecular structure of **1d** and **3** may also contribute to the observed difference in their fluorescence responses toward Zn^{2+} . Calculations at the B3LYP/6-31G* level led to the optimized ground-state structures of **1d** and **3** (Figure S21 in the Supporting Information). The structure shows that **1d** is planar, whereas the 5-(*o*-pyridyl) ring in **3** is slightly twisted from the 2-phenyl-1,3,4-thiodiazole plane. Presumably this could result from a larger repulsion between the S atom and pyridine N atom in **3** than that between the O atom and pyridine N atom in **1d**. The X-ray crystal structure of **1b** (Figure 1) agrees well with the calculated planar structure of **1**. These findings indicate that the O atom in the 1,3,4-oxadiazole group of **1d** possibly acts as the other binding site with Zn^{2+} .

^1H NMR titrations of **1d** by Zn^{2+} and Hg^{2+} in CD_3CN were carried out to better understand the coordination of **1d** with metal ions. The 5-pyridine proton signals of **1d** were affected by the introduction of Zn^{2+} in that the signals of protons *CH1*, *CH2*, *CH3*, and *CH4* shifted significantly (Figure 7). In contrast, all the 2-phenyl protons were only slightly influenced by Zn^{2+} coordination. This titration result clearly confirmed the essential role of the pyridine N atom in its coordination with Zn^{2+} . More importantly, the signals of protons *CH2*, *CH3*, and *CH4* of the 5-pyridyl group shifted significantly downfield upon Zn^{2+} coordination, whereas that of the *CH1* proton at the *ortho* position of the pyridine N atom shifted upfield upon the addition of 0.5 equivalent of Zn^{2+} and thereafter downfield (Figure 7). The shift profile of the *CH1* signal was assumed to result from the initial formation of a 2:1 ligand–metal complex in which the

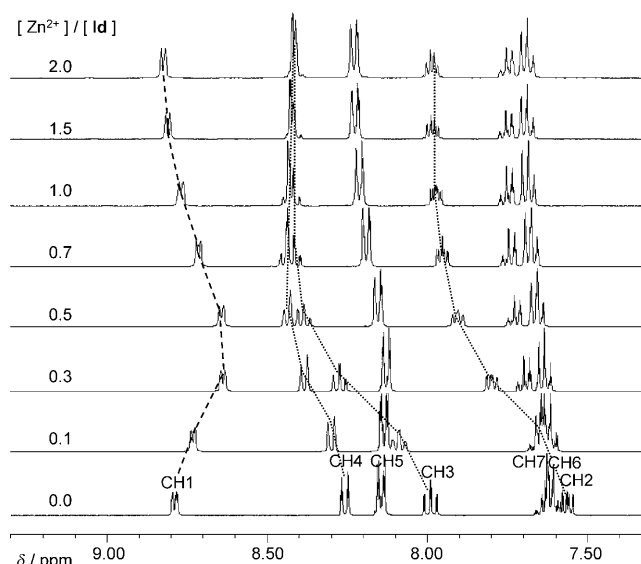
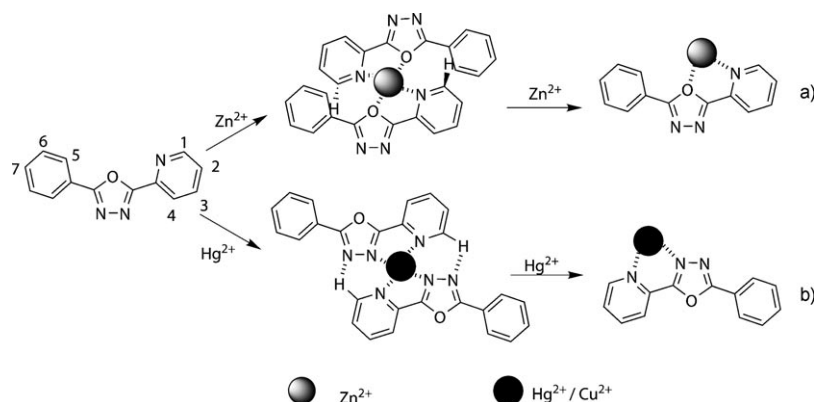


Figure 7. ^1H NMR spectra of **1d** (20 mM) in CD_3CN in the presence of increasing equivalents of $\text{Zn}(\text{ClO}_4)_2$. For proton numbering, see Scheme 2. A possible 2:1 **1d**– Zn^{2+} complex was probed by ^1H NMR spectroscopy, presumably due to the much higher ligand concentration employed here than in the absorption and fluorescence spectral measurements at the $10 \mu\text{M}$ level. Job plots for the **1d**– Zn^{2+} (Cu^{2+}) complex in CH_3CN obtained by monitoring the fluorescence intensity data indicated a 1:1 binding stoichiometry (Figure S22 in the Supporting Information).

CH1 proton was shielded by the aryl ring current of **1d**; at higher Zn^{2+} concentrations, this 2:1 complex decomposed into a 1:1 complex in which no shielding effect existed any more (Scheme 2a). It was therefore made clear that the *CH1* proton behaved differently from others in the 5-pyridyl ring.^[11] This observation helps to probe the coordination of Zn^{2+} with **1d** at its pyridine N atom and oxadiazole O atom. In the case of Hg^{2+} titration, similar downfield shifts in the signals of the *CH2*, *CH3*, and *CH4* protons were observed. The signal of the *CH1* proton, however, behaved oppositely, in that it shifted first to the downfield and then slightly to the upfield (Figure S23 in the Supporting Information). Based on these observations, it was reasonable to conclude that, although the pyridine N atom in **1d** was a binding site



Scheme 2. Proposed coordination modes of **1d** with a) Zn^{2+} and b) Hg^{2+} and Cu^{2+} .

for both Zn^{2+} and Hg^{2+} , the other coordination sites of **1d** with Zn^{2+} and Hg^{2+} differed from each other. It was thus proposed that Hg^{2+} chelated to the pyridine N atom and the 4-N atom in the 1,3,4-oxadiazole moiety of **1d**, as shown in pathway b in Scheme 2. The formation of a 2:1 **1d**- Hg^{2+} complex at a lower equivalent of Hg^{2+} was assigned to be responsible for the downfield shift of the CH1 proton signal, presumably due to an intermolecular hydrogen-bonding interaction between this proton and the 3-N atom of the other oxadiazole moiety. The proposed coordination of **1d** with Cu^{2+} (Scheme 2b) agrees with that of a previously reported relevant complex.^[12]

Logic gating and switching behavior of 1d with metal ions as inputs: Different fluorescence outputs of **1b–e**, in particular **1d**, upon the addition of the tested metal ions Ni^{2+} , Cu^{2+} , Zn^{2+} , Cd^{2+} , Hg^{2+} , and Pb^{2+} provide entries for developing molecular logic gates by using metal ions as inputs. The fluorescence properties of **1d** in the presence and absence of metal inputs were therefore employed to construct molecular logic gates with the fluorescence enhancement factor (I/I_0) as the threshold level. The OR gate is one of the basic logic gates that implement logical disjunction, which results in a high output (1) if one or both inputs to the gate are high (1).^[13] The fluorescence of **1d** ($10\ \mu\text{M}$), which can be enhanced by Zn^{2+} or Cd^{2+} or both, enables the OR logic function when 1 equivalent of Zn^{2+} ($10\ \mu\text{M}$) and 5 equivalents of Cd^{2+} ($50\ \mu\text{M}$) are taken as inputs (Figure 8).

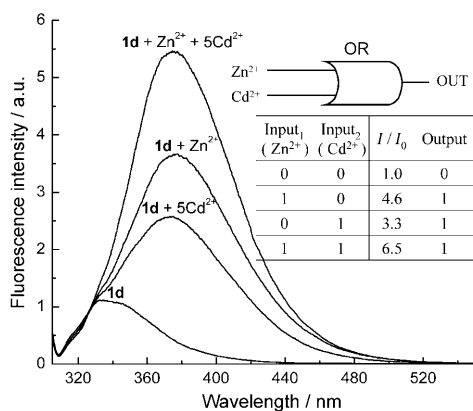


Figure 8. Fluorescence spectra of **1d** ($10\ \mu\text{M}$) in CH_3CN in the presence of chemical inputs. $[\text{Zn}^{2+}] = 10\ \mu\text{M}$, $[\text{Cd}^{2+}] = 50\ \mu\text{M}$. The excitation wavelength was 300 nm. The inset shows the logic table and the respective symbolic representation of the OR function. I/I_0 is the ratio of the fluorescence spectrum area (310–520 nm) in the presence of metal ion to that in the absence of the metal ion.

The NOR gate, as a universal gate that allows the combinatorial creation of all other Boolean operations, is of potential interest.^[14] A NOR gate, which integrates NOT and OR logic gates, is performed only when neither of two inputs is present. The combination of metal ions Ni^{2+} , Cu^{2+} , Hg^{2+} , and Pb^{2+} as inputs leads to fluorescence quenching of **1d**, and expresses the NOR logic function. The level of fluo-

rescence intensity of **1d** ($10\ \mu\text{M}$) as a function of 5 equivalents of Cu^{2+} ($50\ \mu\text{M}$) and 5 equivalents of Hg^{2+} ($50\ \mu\text{M}$) as inputs is read as a NOR logic response. The truth table presented in Figure 9 indicates that the fluorescence of **1d** ap-

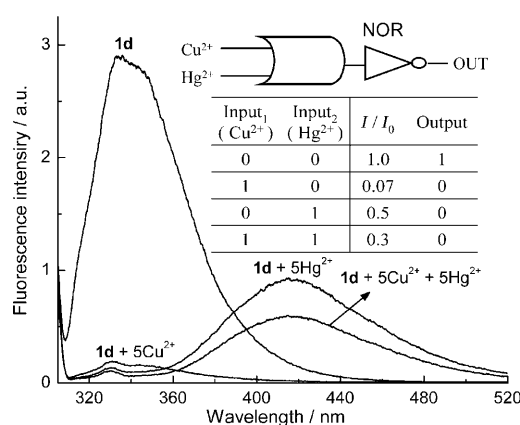


Figure 9. Fluorescence spectra of **1d** ($10\ \mu\text{M}$) in CH_3CN in the presence of chemical inputs. $[\text{Cu}^{2+}] = [\text{Hg}^{2+}] = 50\ \mu\text{M}$. The excitation wavelength was 300 nm. The inset shows the logic table and the respective symbolic representation of the NOR function.

pears at 334 nm (output “1”) when neither Cu^{2+} nor Hg^{2+} is added, whereas it is quenched by applying one or both inputs, which affords output “0”.

The INHIBIT gate can be interpreted as a particular integration of AND and NOT logic gates such that the output signal is inhibited by one of the active inputs.^[15] A basic two-input INHIBIT action can be obtained for **1d** ($10\ \mu\text{M}$) with Zn^{2+} ($10\ \mu\text{M}$) and Cu^{2+} ($50\ \mu\text{M}$) as inputs. Enhancement of **1d** fluorescence is observed only in the presence of 1 equivalent of Zn^{2+} and the absence of Cu^{2+} , so that the output is read as “1”. Under other circumstances the fluorescence of **1d** is quenched, thus leading to output “0”. The corresponding truth table for the INHIBIT function is illustrated in Figure 10. It was therefore made clear that the IN-

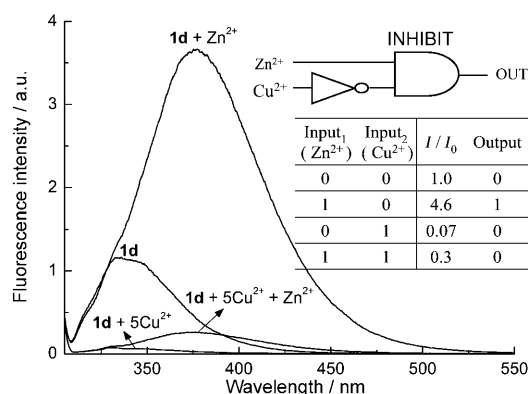


Figure 10. Fluorescence spectra of **1d** ($10\ \mu\text{M}$) in CH_3CN in the presence of chemical inputs. $[\text{Zn}^{2+}] = 10\ \mu\text{M}$, $[\text{Cu}^{2+}] = 50\ \mu\text{M}$. The excitation wavelength was 300 nm. The inset shows the logic table and the respective symbolic representation of the INHIBIT function.

HIBIT function could be expanded to an enabled NOR (EnNOR) logic gate by combining a NOR operator.^{[6], [16]} Here, Zn^{2+} is a controlling input, which means that whenever it is “1” the NOR gate works whereas this gate closes if it is “0”. The corresponding logic circuit is depicted in Figure 11b.

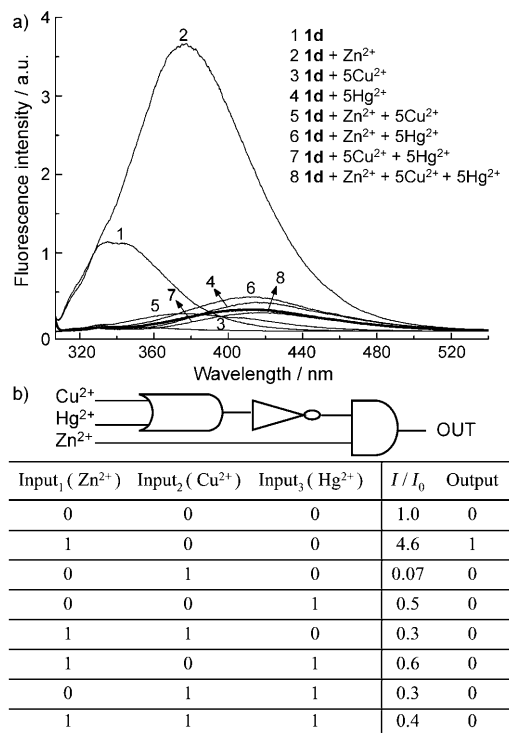


Figure 11. a) Fluorescence spectra of **1d** (10 μ M) in CH_3CN in the presence of chemical inputs. [Zn^{2+}] = 10 μ M, [Cu^{2+}] = [Hg^{2+}] = 50 μ M. b) The logic table and respective symbolic representation of the EnNOR function. The excitation wavelength was 300 nm.

The rich fluorescence response profiles of **1d** toward Zn^{2+} and Cu^{2+} also make it feasible to build up fluorescent switches.^[17] The fluorescence of **1d** in CH_3CN was enhanced upon addition of Zn^{2+} , whereas it was significantly quenched by Cu^{2+} . Therefore, the fluorescent “ON” and “OFF” states can be modulated by the relative concentration of Zn^{2+} and Cu^{2+} . By setting $I/I_0 > 2.0$ as the threshold for the fluorescent “ON” state and $I/I_0 < 0.5$ as that for the fluorescent “OFF” state, the fluorescent “ON” and “OFF” states can be established by alternate addition of Zn^{2+} and Cu^{2+} . Sequential titration of **1d** by Zn^{2+} and Cu^{2+} caused the fluorescence to be enhanced (ON) and quenched (OFF) (Figure 12). The fluorescent switches resulted from the competitive coordination of Zn^{2+} and Cu^{2+} with **1d** that formed **1d**- Zn^{2+} and/or **1d**- Cu^{2+} .

Conclusion

2,5-Diaryl-1,3,4-oxadiazoles bearing a 2-(*para*-substituted)-phenyl and a 5-(*o*-pyridyl) group (substituent X = NMe_2 , OEt, Me, H, and Cl; **1a–e**) were designed for fluorescent

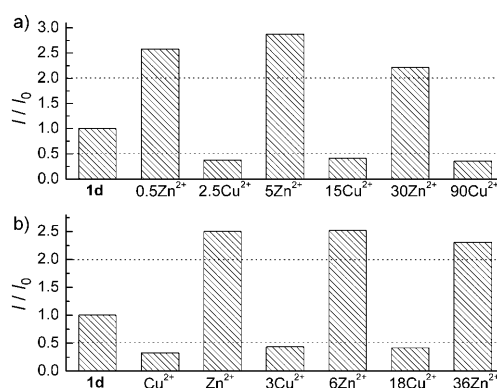


Figure 12. Outputs (I/I_0) of **1d** (10 μ M) in CH_3CN upon alternate addition of Zn^{2+} and Cu^{2+} : a) 5.0 μ M Zn^{2+} , 25.0 μ M Cu^{2+} , 50.0 μ M Zn^{2+} , 150.0 μ M Cu^{2+} , 300.0 μ M Zn^{2+} , 900.0 μ M Cu^{2+} and b) 10.0 μ M Cu^{2+} , 10.0 μ M Zn^{2+} , 30.0 μ M Cu^{2+} , 60.0 μ M Zn^{2+} , 180.0 μ M Cu^{2+} , 360.0 μ M Zn^{2+} . The excitation wavelength was 300 nm.

logic gates and switches. By modifying the substituent X at the 2-phenyl group, we demonstrated that the electronic distribution and the emissive state of the molecule can be modulated and that the emission depended sensitively on the electronic distribution. The 5-(*o*-pyridyl) group was incorporated to form a bidentate coordination environment with a 1,3,4-oxadiazole core, which creates two distinct coordination modes for binding with different metal ions. 2,5-Diaryl-1,3,4-oxadiazoles were shown to exhibit fluorescence response profiles varying in both intensity and wavelength toward metal ions such as Ni^{2+} , Cu^{2+} , Zn^{2+} , Cd^{2+} , Hg^{2+} , and Pb^{2+} . This provides access to establish multiple logic functions in a single molecular system. OR, NOR, INHIBIT, and EnNOR logic gates as well as “ON-OFF-ON” and “OFF-ON-OFF” fluorescent switches were accordingly constructed from one derivative (**1d**) by varying the combinations and levels of metal-ion inputs. It is expected that structural modifications on 2- and/or 5-aryl moieties would create more structural motifs for extended design and applications in molecular “intelligence”, which is now under way in this laboratory.

Experimental Section

Materials: Chemicals used for synthesis were commercially available. CH_3CN was of HPLC quality. CHX, DEE, EtOAc, CH_2Cl_2 , and CH_3CN for spectral studies were redistilled. Metal ions were used as their perchlorates. Solvents for NMR measurements had a deuteration grade of > 99 atom D%. Compounds **1d**,^[18] **1e**,^[19] **2**,^[18] and **3**^[20] have been reported in the literature.

Measurements and methods: Absorption and fluorescence spectra were recorded in a 1 cm quartz cell. All spectral titrations were carried out by keeping the concentration of **1–3** constant (10 μ M) while varying the metal-ion concentrations (0–250 μ M). The binding constants K_s were determined from the absorbance in CH_3CN at 25 °C. The absorbance data were fitted to Equation (1),^[9] in which A is the absorbance of the ligand in the presence of a given amount of metal ion, A_0 is the absorbance of the initial solution of the free ligand, A_{limit} is the absorbance of full complexation, and C_0 and C_M are the molar concentrations of ligand and

metal ion, respectively. Fluorescence quantum yields were measured using quinine sulfate as a standard (0.546 in 0.5 M H₂SO₄).^[10]

$$A = A_0 + \frac{A_{\text{limit}} - A_0}{2c_0} \left[c_M + 1/K_s + c_0 - \sqrt{(c_M + 1/K_s + c_0)^2 - 4c_0c_M} \right] \quad (1)$$

¹H NMR (500 MHz) and ¹³C NMR (100 MHz) spectra were recorded in CDCl₃ with TMS as an internal standard. ¹H NMR (400 MHz) titrations of **1d** by Zn²⁺ and Hg²⁺ were carried out in CD₃CN. HRMS spectra were obtained by using methanol as the solvent.

Single-crystal X-ray diffraction data were collected at 273 K. Absorption corrections were applied by using the multiscan program SADABS. The structure was solved by direct methods, and non-hydrogen atoms were refined anisotropically by a least-squares method on *F*² by using the SHELXTL-97 program. The hydrogen atoms were generated geometrically (C–H, 0.96 Å). CCDC-745239 (**1b**) contains the supplementary crystallographic data for this paper. These data can be obtained free of charge from The Cambridge Crystallographic Data Centre via www.ccdc.cam.ac.uk/data_request/cif.

Geometry optimizations and vibrational analysis were performed by density functional theory with Becke's three-parameter hybrid exchange functional and the Lee–Yang–Parr correlation functional (B3LYP) implemented in the Gaussian 03 package. The 6-31G* basis set was used in all calculations.

Preparation and characterization of 1–3: The substituted benzoyl chloride (2.2 mmol) in CH₂Cl₂ (10 mL) was added dropwise to a dried round flask containing picolinohydrazine or benzoyl hydrazine (2.0 mmol), pyridine (1.0 mL), and *N,N*-dimethyl-4-aminopyridine (DMAP; 60 mg) in dichloromethane (15 mL). The mixture was stirred at room temperature for 6 h and then washed with dilute aqueous HCl (1 M, 3 × 10 mL) and water (3 × 10 mL), and dried over sodium sulfate. After removal of the solvent at reduced pressure, *N'*-(4-substituted-benzoyl)picolinohydrazide or *N'*-benzoylbenzohydrazide was obtained as a white solid in 85% yield, and was directly used for the next step.

1 and **2** were respectively synthesized from *N'*-(4-substituted-benzoyl)picolinohydrazide and *N'*-benzoylbenzohydrazide (1.5 mmol) by heating its POCl₃ (10 mL) solution at reflux for 6 h. After cooling, the solution was poured into iced water and neutralized with saturated NaHCO₃ solution. The resulting solution was extracted with CHCl₃ (3 × 15 mL) and the organic phase was washed with water (3 × 15 mL) and saturated NaHCO₃ solution (3 × 15 mL), and dried over sodium sulfate. After evaporation of the solvent under reduced pressure, the residue was subjected to column chromatography on silica gel (ethyl acetate/petroleum ether, 1:3) to afford **1** or **2** in 75–80% yield.

Compound **3** was synthesized by heating the solution of *N'*-benzoylpicolinohydrazide (1.5 mmol) and P₂S₅ (8 equiv) in pyridine (20 mL) to reflux. After evaporation of the solvent under reduced pressure, water (30 mL) was added and the mixture was extracted with CH₂Cl₂ (3 × 10 mL). The CH₂Cl₂ phase was washed with KOH (1 M, 3 × 10 mL) and then HCl (1 M, 3 × 10 mL), and dried over sodium sulfate. The solvent was removed under reduced pressure, and the crude product was purified by column chromatography on silica gel (ethyl acetate/petroleum ether, 1:4) to afford **3** as a white solid in 60% yield.

2-(4-Dimethylamino)-5-(pyridin-2-yl)-1,3,4-oxadiazole (1a): ¹H NMR (500 MHz, CDCl₃, TMS): δ = 3.07 (s, 6H), 6.75 (d, *J* = 9.0 Hz, 2H), 7.42–7.45 (m, 1H), 7.85–7.89 (m, 1H), 8.06 (d, *J* = 9.0 Hz, 2H), 8.29 (d, *J* = 8.0 Hz, 1H), 8.79–8.81 ppm (m, 1H); ¹³C NMR (100 MHz, CDCl₃, TMS): δ = 40.0, 110.6, 111.5, 122.9, 125.3, 128.7, 137.0, 144.1, 150.1, 152.6, 162.8, 166.3 ppm; HRMS (ESI): *m/z*: calcd for C₁₅H₁₅N₄O: 267.1246 [M+H⁺]; found: 267.1241 [M+H⁺].

2-(4-Ethoxyphenyl)-5-(pyridin-2-yl)-1,3,4-oxadiazole (1b): ¹H NMR (500 MHz, CDCl₃, TMS): δ = 1.46 (t, *J* = 7.0 Hz, 3H), 4.12 (q, *J* = 7.0 Hz, 2H), 7.01 (d, *J* = 9.0 Hz, 2H), 7.45–7.47 (m, 1H), 7.88–7.91 (m, 1H), 8.14 (d, *J* = 9.0 Hz, 2H), 8.30 (d, *J* = 8.0 Hz, 1H), 8.80–8.82 ppm (m, 1H); ¹³C NMR (100 MHz, CDCl₃, TMS): δ = 14.7, 63.8, 114.9, 115.9, 123.1, 125.6, 129.1, 137.1, 143.9, 150.2, 162.0, 163.4, 165.6 ppm; HRMS (ESI): *m/z*: calcd for C₁₅H₁₄N₄O₂: 268.1086 [M+H⁺]; found: 268.1083 [M+H⁺].

2-*p*-Tolyl-5-(pyridin-2-yl)-1,3,4-oxadiazole (1c): ¹H NMR (500 MHz, CDCl₃, TMS): δ = 2.44 (s, 3H), 7.33 (d, *J* = 8.0 Hz, 2H), 7.46 (t, *J* = 6.0 Hz, 1H), 7.89 (t, *J* = 8.0 Hz, 1H), 8.10 (d, *J* = 7.0 Hz, 2H), 8.31 (d, *J* = 8.0 Hz, 1H), 8.81 ppm (d, *J* = 4.5 Hz, 1H); ¹³C NMR (100 MHz, CDCl₃, TMS): δ = 21.6, 120.8, 123.1, 125.7, 127.2, 129.7, 137.1, 142.6, 143.7, 150.2, 163.6, 165.7 ppm; HRMS (ESI): *m/z*: calcd for C₁₄H₁₂N₄O: 238.0980 [M+H⁺]; found: 238.0983 [M+H⁺].

2-Phenyl-5-(pyridin-2-yl)-1,3,4-oxadiazole (1d): ¹H NMR (500 MHz, CDCl₃, TMS): δ = 7.47–7.49 (m, 1H), 7.52–7.57 (m, 3H), 7.89–7.93 (m, 1H), 8.22–8.24 (m, 2H), 8.32 (d, *J* = 8.0 Hz, 1H), 8.82–8.83 ppm (m, 1H); ¹³C NMR (100 MHz, CDCl₃, TMS): δ = 123.3, 123.7, 125.8, 127.3, 129.0, 132.0, 137.2, 143.7, 150.3, 163.9, 165.6 ppm; HRMS (ESI): *m/z*: calcd for C₁₃H₁₀N₄O: 224.0824 [M+H⁺]; found: 224.0817 [M+H⁺].

2-(4-Chlorophenyl)-5-(pyridin-2-yl)-1,3,4-oxadiazole (1e): ¹H NMR (500 MHz, CDCl₃, TMS): δ = 7.47–7.50 (m, 1H), 7.52 (d, 2H, *J* = 9.0 Hz, 2H), 7.89–7.93 (m, 1H), 8.16 (d, *J* = 8.5 Hz, 2H), 8.32 (d, *J* = 7.5 Hz, 1H), 8.82 ppm (d, *J* = 4.5 Hz, 1H); ¹³C NMR (100 MHz, CDCl₃, TMS): δ = 122.1, 123.3, 125.9, 128.5, 129.4, 137.2, 138.3, 143.5, 150.3, 164.0, 164.8 ppm; HRMS (ESI): *m/z*: calcd for C₁₃H₉ClN₄O: 258.0434 [M+H⁺]; found: 258.0434 [M+H⁺].

2,5-Diphenyl-1,3,4-oxadiazole (2): ¹H NMR (500 MHz, CDCl₃, TMS): δ = 7.52–7.57 (m, 6H), 8.14–8.16 ppm (m, 4H); ¹³C NMR (100 MHz, CDCl₃, TMS): δ = 123.9, 126.9, 129.1, 131.7, 164.6 ppm; HRMS (ESI): *m/z*: calcd for C₁₄H₁₁N₂O: 223.0871 [M+H⁺]; found: 223.0875 [M+H⁺].

2-Phenyl-5-(pyridin-2-yl)-1,3,4-thiadiazole (3): ¹H NMR (500 MHz, CDCl₃, TMS): δ = 7.39–7.41 (m, 1H), 7.51–7.52 (m, 3H), 7.87 (t, *J* = 8.0 Hz, 1H), 8.05 (t, *J* = 3.5 Hz, 2H), 8.40 (d, *J* = 8.0 Hz, 1H), 8.68 ppm (d, *J* = 5.0 Hz, 1H); ¹³C NMR (100 MHz, CDCl₃, TMS): δ = 121.0, 125.3, 128.0, 129.2, 130.3, 131.2, 137.2, 149.2, 149.8, 169.9, 170.0 ppm; HRMS (ESI): *m/z*: calcd for C₁₃H₁₀N₃S: 240.0595 [M+H⁺]; found: 240.0590 [M+H⁺].

Acknowledgements

This work was supported by the NSFC of China through grant nos. J0630429, 20675069, and 20835005.

- [1] V. Balzani, A. Credi, F. M. Raymo, J. F. Stoddart, *Angew. Chem.* **2000**, *112*, 3484–3530; *Angew. Chem. Int. Ed.* **2000**, *39*, 3348–3391.
- [2] a) J. Andréasson, U. Pischel, *Chem. Soc. Rev.* **2010**, *39*, 174–188; b) K. Szacilowski, *Chem. Rev.* **2008**, *108*, 3481–3548; c) U. Pischel, *Angew. Chem.* **2007**, *119*, 4100–4115; *Angew. Chem. Int. Ed.* **2007**, *46*, 4026–4040; d) A. P. de Silva, S. Uchiyama, *Nat. Nanotechnol.* **2007**, *2*, 399–410; e) A. P. de Silva, N. D. McClenaghan, *Chem. Eur. J.* **2004**, *10*, 574–586; f) F. M. Raymo, *Adv. Mater.* **2002**, *14*, 401–414; g) A. P. de Silva, N. D. McClenaghan, *Chem. Eur. J.* **2002**, *8*, 4935–4945.
- [3] A. P. de Silva, H. Q. N. Gunaratne, C. P. McCoy, *Nature* **1993**, *364*, 42–44.
- [4] For reviews, see: a) A. P. de Silva, T. P. Vance, M. E. S. West, G. D. Wright, *Org. Biomol. Chem.* **2008**, *6*, 2468–2480; b) A. Credi, *Angew. Chem.* **2007**, *119*, 5568–5572; *Angew. Chem. Int. Ed.* **2007**, *46*, 5472–5475; c) D. C. Magri, T. P. Vance, A. P. de Silva, *Inorg. Chim. Acta* **2007**, *360*, 751–764; d) V. Balzani, A. Credi, M. Venturi, *ChemPhysChem* **2003**, *4*, 49–59; e) G. J. Brown, A. P. de Silva, S. Pagliari, *Chem. Commun.* **2002**, 2461–2463; f) A. P. de Silva, I. M. Dixon, H. Q. N. Gunaratne, T. Gunnlaugsson, P. R. S. Maxwell, T. E. Rice, *J. Am. Chem. Soc.* **1999**, *121*, 1393–1394.
- [5] For some latest papers, see: a) P. Remón, R. Ferreira, J. M. Montenegro, R. Suau, E. Pérez-Inestrosa, U. Pischel, *ChemPhysChem* **2009**, *10*, 2004–2007; b) L. Mu, W. Shi, G. She, J. C. Chang, S. T. Lee, *Angew. Chem.* **2009**, *121*, 3521–3524; *Angew. Chem. Int. Ed.* **2009**, *48*, 3469–3472; c) R. Ferreira, P. Remón, U. Pischel, *J. Phys. Chem. C* **2009**, *113*, 5805–5811; d) N. Kaur, N. Singh, D. Cairns, J. F.

- Callan, *Org. Lett.* **2009**, *11*, 2229–2232; e) Z. Guo, P. Zhao, W. Zhu, X. Huang, Y. Xie, H. Tian, *J. Phys. Chem. C* **2008**, *112*, 7047–7053; f) G. Zong, G. Lu, *Tetrahedron Lett.* **2008**, *49*, 5676–5679; g) X. Chen, Z. Li, Y. Xiang, A. Tong, *Tetrahedron Lett.* **2008**, *49*, 4697–4700.
- [6] a) G. Q. Zong, G. X. Lu, *J. Phys. Chem. C* **2009**, *113*, 2541–2546; b) S. Kumar, V. Luxami, R. Saini, D. Kaur, *Chem. Commun.* **2009**, 3044–3046; c) C. H. Xu, W. Sun, Y. R. Zheng, C. J. Fang, C. Zhou, J. Y. Jin, C. H. Yan, *New J. Chem.* **2009**, *33*, 838–846; d) Z. X. Li, L. Y. Liao, W. Sun, C. H. Xu, C. Zhang, C. J. Fang, C. H. Yan, *J. Phys. Chem. C* **2008**, *112*, 5190–5196; e) D. Zhang, J. H. Su, X. Ma, H. Tian, *Tetrahedron* **2008**, *64*, 8515–8521; f) U. Pischel, B. Heller, *New J. Chem.* **2008**, *32*, 395–400; g) D. Margulies, C. E. Felder, G. Melman, A. Shanzer, *J. Am. Chem. Soc.* **2007**, *129*, 347–354; h) C. J. Fang, Z. Zhu, W. Sun, C. H. Xu, C. H. Yan, *New J. Chem.* **2007**, *31*, 580–586; i) W. Sun, Y. R. Zheng, C. H. Xu, C. J. Fang, C. H. Yan, *J. Phys. Chem. C* **2007**, *111*, 11706–11711; j) P. Singh, S. Kumar, *New J. Chem.* **2006**, *30*, 1553–1556; k) Y. Shiraishi, Y. Tokitoh, T. Hirai, *Chem. Commun.* **2005**, 5316–5318; l) S. H. Lee, J. Y. Kim, S. K. Kim, J. H. Lee, J. S. Kim, *Tetrahedron* **2004**, *60*, 5171–5176; m) S. Alves, F. Pina, M. T. Albelda, E. García-España, C. Soriano, S. V. Luis, *Eur. J. Inorg. Chem.* **2001**, 405–412.
- [7] a) F. A. Khan, K. Parasuraman, K. K. Sadhu, *Chem. Commun.* **2009**, 2399–2401; b) Z. Q. Guo, W. H. Zhu, L. J. Shen, H. Tian, *Angew. Chem.* **2007**, *119*, 5645–5649; *Angew. Chem. Int. Ed.* **2007**, *46*, 5549–5553; c) A. Petitjean, N. Kyritsakas, J. M. Lehn, *Chem. Eur. J.* **2005**, *11*, 6818–6828; d) K. Rurack, A. Koval'chuck, J. L. Bricks, J. L. Slobinskii, *J. Am. Chem. Soc.* **2001**, *123*, 6205–6206.
- [8] a) Y. Liu, L. L. Zong, L. F. Zheng, L. G. Wu, Y. X. Cheng, *Polymer* **2007**, *48*, 6799–6807; b) C. K. Kwak, C. H. Lee, T. S. Lee, *Tetrahedron Lett.* **2007**, *48*, 7788–7792; c) S. H. Mashraqui, S. Sundaram, A. C. Bhasikuttan, *Tetrahedron* **2007**, *63*, 1680–1688; d) G. Zhou, Y. X. Cheng, L. X. Wang, X. B. Jing, F. S. Wang, *Macromolecules* **2005**, *38*, 2148–2153.
- [9] B. Valeur, J. Pouget, J. Bourson, M. Kaschke, N. P. Ersting, *J. Phys. Chem.* **1992**, *96*, 6545–6549.
- [10] J. N. Demas, G. A. Crosby, *J. Phys. Chem.* **1971**, *75*, 991–1024.
- [11] a) Ö. A. Bozdemir, O. Büyükcakir, E. U. Akkaya, *Chem. Eur. J.* **2009**, *15*, 3830–3838; b) R. Dobrawa, M. Lysetska, P. Ballester, M. Grüne, F. Würthner, *Macromolecules* **2005**, *38*, 1315–1325.
- [12] P. Gómez-Saiz, J. García-Tojal, F. J. Arnáiz, M. A. Maestro, L. Lezama, T. Rojo, *Inorg. Chem. Commun.* **2003**, *6*, 558–560.
- [13] a) H. J. Jung, N. Singh, D. Y. Lee, D. O. Jang, *Tetrahedron Lett.* **2009**, *50*, 5555–5558; b) G. McSkimming, J. H. R. Tucker, H. Bouas-Laurent, J. P. Desvergne, *Angew. Chem.* **2000**, *112*, 2251–2253; *Angew. Chem. Int. Ed.* **2000**, *39*, 2167–2169; c) P. Ghosh, P. K. Bharadwaj, S. Mandal, S. Ghosh, *J. Am. Chem. Soc.* **1996**, *118*, 1553–1554.
- [14] a) A. Dhir, V. Bhalla, M. Kumar, *Org. Lett.* **2008**, *10*, 4891–4894; b) M. Biancardo, C. Bignozzi, H. Doyle, G. Redmond, *Chem. Commun.* **2005**, 3918–3920; c) Z. Wang, G. Zheng, P. Lu, *Org. Lett.* **2005**, *7*, 3669–3672; d) B. Turfan, E. U. Akkaya, *Org. Lett.* **2002**, *4*, 2857–2859.
- [15] a) M. J. Yuan, W. D. Zhou, X. F. Liu, M. Zhu, J. B. Li, X. D. Yin, H. Y. Zheng, Z. C. Zuo, C. B. Ouyang, H. B. Liu, Y. L. Li, D. B. Zhu, *J. Org. Chem.* **2008**, *73*, 5008–5014; b) A. Dhir, V. Bhalla, M. Kumar, *Tetrahedron Lett.* **2008**, *49*, 4227–4230; c) M. Kluciar, R. Ferreira, B. de Castro, U. Pischel, *J. Org. Chem.* **2008**, *73*, 6079–6085; d) G. Nishimura, K. Ishizumi, Y. Shiraishi, T. Hirai, *J. Phys. Chem. B* **2006**, *110*, 21596–21602; e) H. Miyaji, H. K. Kim, E. K. Sim, C. K. Lee, W. S. Cho, J. L. Sessler, C. H. Lee, *J. Am. Chem. Soc.* **2005**, *127*, 12510–12512.
- [16] M. de Sousa, B. de Castro, S. Abad, M. A. Miranda, U. Pischel, *Chem. Commun.* **2006**, 2051–2053.
- [17] a) M. Kumar, R. Kumar, V. Bhalla, *Chem. Commun.* **2009**, 7384–7386; b) D. Zhang, Q. Zhang, J. Su, H. Tian, *Chem. Commun.* **2009**, 1700–1702; c) S. H. Kim, J. S. Kim, S. M. Park, S. K. Chang, *Org. Lett.* **2006**, *8*, 371–374; d) S. H. Kim, J. K. Choi, S. K. Kim, W. Sim, J. S. Kim, *Tetrahedron Lett.* **2006**, *47*, 3737–3741.
- [18] Yu. A. Efimova, T. V. Artamonova, G. I. Koldobskii, *Russ. J. Org. Chem.* **2008**, *44*, 1345–1347.
- [19] D. M. Pore, S. M. Mahadik, U. V. Desai, *Synth. Commun.* **2008**, *38*, 3121–3128.
- [20] M. Santus, *Acta Pol. Pharm.* **1988**, *45*, 219–224.

Received: November 30, 2009
Published online: April 9, 2010